Biogeosciences Discuss., https://doi.org/10.5194/bg-2017-177
Manuscript under review for journal Biogeosciences
Discussion started: 20 June 2017

Biogeosciences Discussions Open Access EGU

How big is the influence of biogenic silicon pools on short-term changes of water soluble silicon in soils? Implications from a study of a ten-year-old plant-soil-system

Daniel Puppe[a,*], **Axel Höhn**[a], **Danuta Kaczorek**[b], **Manfred Wanner**[c], **Marc Wehrhan**[a], **Michael Sommer**[a,d]

[a] Leibniz-Centre for Agricultural Landscape Research (ZALF) e.V., Institute of Soil Landscape Research, 15374 Müncheberg, Germany

[b] Department of Soil Environment Sciences, Warsaw University of Life Science (SGGW), Nowoursynowska 159, 02-776 Warsaw, Poland

[c] Brandenburg University of Technology Cottbus-Senftenberg, Department Ecology, 03013 Cottbus, Germany

[d] University of Potsdam, Institute of Earth and Environmental Sciences, 14476 Potsdam, Germany

* Corresponding author. E-mail address: daniel.puppe@zalf.de

Abstract

The significance of biogenic silicon (BSi) pools as a key factor for the control of Si fluxes from terrestrial to aquatic ecosystems has been recognized since decades. However, while most research has been focused on phytogenic Si pools, knowledge on other BSi pools is still limited. We hypothesized different BSi pools to influence short-term changes of the water soluble Si fraction in soils to different extents. To test our hypothesis we took plant (*Calamagrostis epigejos*, *Phragmites australis*) and soil samples in an artificial catchment in a post-mining landscape in the state of Brandenburg, Germany. We quantified phytogenic

(phytoliths), protistic (diatom frustules and testate amoeba shells) and zoogenic (sponge spicules) Si pools as well as Tiron extractable and water soluble Si fractions in soils at the beginning (t_0) and after ten years (t_{10}) of ecosystem development. As expected the results of Tiron extraction showed, that there are no consistent changes of the amorphous Si pool at 'Chicken Creek' as early as after ten years. In contrast, compared to t_0 we found increased water soluble Si and BSi pools at t_{10}, thus we concluded BSi pools to be the main driver of short-term changes of water soluble Si. However, because total BSi represents only small proportions of water soluble Si at t_0 (<2 %) and t_{10} (2.8-4.3 %) we further concluded smaller (<5 µm) and fragile phytogenic Si structures to have the biggest impact on short-term changes of water-soluble Si. In this context, phytoliths (>5 µm) only amounted to about 16 % of total Si contents of plant materials of *C. epigejos* and *P. australis* at t_{10}, thus about 84 % of small-scale and fragile phytogenic Si are not quantified by the used phytolith extraction. Analyses of small-scale and fragile phytogenic Si structures are urgently needed in future work as they seem to represent the biggest and most reactive Si pool in soils, thus the most important driver of Si cycling in terrestrial biogeosystems.

Keywords

biosilicification, initial biogeosystem, phytogenic Si, protistic Si, zoogenic Si

Biogeosciences Discuss., https://doi.org/10.5194/bg-2017-177
Manuscript under review for journal Biogeosciences
Discussion started: 20 June 2017

1. Introduction

Various prokaryotes and eukaryotes are able to synthesize hydrated amorphous silica ($SiO_2 \cdot nH_2O$) structures from monomeric silicic acid (H_4SiO_4), a process called biosilicification (Ehrlich et al. 2010). In terrestrial biogeosystems biogenic silicon (BSi) synthesized by bacteria and fungi, plants, diatoms, testate amoebae and sponges can be found forming corresponding microbial, phytogenic, protophytic, protozoic and zoogenic BSi pools, respectively (Puppe et al. 2015, Sommer et al. 2006). BSi has been recognized as a key factor for the control of Si fluxes from terrestrial to aquatic ecosystems as it is in general more soluble compared to silicate minerals (e.g., Fraysse et al. 2006, 2009). These fluxes influence marine diatom production on a global scale (Dürr et al. 2011, Sommer et al. 2006, Struyf & Conley 2012). Marine diatoms in turn can fix large quantities of carbon dioxide via photosynthesis because up to 54 % of the biomass in the oceans is represented by diatoms, thus diatoms have an important influence on climate change (Tréguer & De La Rocha 2013, Tréguer & Pondaven 2000).

While the importance of phytogenic Si pools for global Si fluxes has been recognized for three decades (e.g., Bartoli 1983, Meunier et al. 1999, Street-Perrott & Barker 2008), information on the other BSi pools is comparably rare (Clarke 2003). However, in recent publications the potential importance of diatoms, testate amoebae and sponge spicules in soils for Si cycling has been highlighted (Aoki et al. 2007, Creevy et al. 2016, Puppe et al. 2014, 2015, 2016). Furthermore, evidence arises that BSi pools are in disequilibrium at decadal time scales due to disturbances and perturbations by humans, e.g., by changes in forest management or farming practices (Barão et al. 2014, Keller et al. 2012, Vandevenne et al. 2015). In consequence, BSi accumulation and BSi dissolution are not balanced, which influences Si cycling in terrestrial biogeosystems not only on decadal but also on millennial

scales (Clymans et al. 2011, Frings et al. 2014, Sommer et al. 2013, Struyf et al. 2010). Sommer et al. (2013), for example, found the successive dissolving of a relict phytogenic Si pool to be the main source of dissolved Si in soils of a forested biogeosystem. Due to the fact that the continuous decomposition of this relict phytogenic Si pool is not compensated by an equivalent buildup by recent vegetation the authors concluded a BSi disequilibrium on a decadal scale. On a millennial scale Clymans et al. (2011) estimated the total amorphous Si storage in temperate soils to be drecreased by approximately 10 % since the onset of agricultural development about 5,000 years ago. This decrease not only has consequences for land-ocean Si fluxes but also influences agricultural used landscapes because Si is a beneficial element for many crops (e.g., Epstein 2009, Ma & Yamaji 2008).

For a better understanding of BSi dynamics, chronosequence studies are well suited, because they allow us to analyze time-related changes of BSi pools during biogeosystem development. In the present study we analyzed various BSi pools in differently aged soils of an initial artificial catchment ('Chicken Creek') in a post-mining landscape in NE Germany. Chicken Creek represents a study site with defined initial conditions and offers the rare opportunity to monitor BSi dynamics from the very beginning. Former studies at this site revealed i) a formation of protophytic (diatom frustules), protozoic (testate amoeba shells) and zoogenic (sponge spicules) Si pools within a short time (<10 years) and ii) a strong relation of spatiotemporal changes of protistic (diatoms and testate amoebae) BSi pools to the vegetation, because plants provide, e.g., rhizospheric micro-habitats including enhanced food supply (Puppe et al. 2014, 2016). From these results it can be concluded that especially vegetated spots at initial biogeosystem sites represent hot spots of BSi accumulation of various origin (compare Wanner & Elmer 2009). Furthermore, construction work with large machines resulted in differently structured sections of Chicken Creek with slight differences

in abiotic conditions (for details see subsection 2.1.) (Gerwin et al. 2010). These differences in turn lead to section-specific vegetation dynamics at Chicken Creek (Zaplata et al. 2010). Knowledge about BSi accumulation dynamics is crucial for the understanding of Si cycling in terrestrial biogeosystems. We regard water extractable Si as an useful proxy for desilication and biological uptake (plants, testate amoebae etc.). In addition, we used an alkaline extractant (Tiron) to detect eventual short-term changes of the amorphous Si fraction. We hypothesized i) BSi pools to influence short-term changes of water soluble Si in initial soils, but no short-term changes in amorphous Si fractions, ii) the phytogenic Si pool to be the most prominent one in size, thus the biggest driver of short-term changes of water soluble Si, and iii) BSi pool changes to be section-specific, i.e., related to vegetation dynamics. The aims of the present study were i) to quantify various BSi pools, i.e., protophytic, protozoic, zoogenic and phytogenic Si pools, during initial soil and ecosystem development, (ii) to analyze potential section-specific short-term changes of these BSi pools after a decade of ecosystem development, and iii) to evaluate the influence of different BSi pools on water soluble Si in these soils.

2. Material and methods

2.1. Study site

The study site Chicken Creek (51°36'18" N, 14°15'58" E) represents an artificial catchment in a post-mining landscape located in the active mining area 'Welzow-South' (lignite open-cast mining, 150 km south-east of Berlin) in the state of Brandenburg, Germany (Kendzia et al. 2008, Russell et al. 2010). Climate at Chicken Creek is characterized by an average air temperature of 9.6°C and an annual precipitation of 568 mm comprising data from 1981 to 2010 (Meteorological Station Cottbus, German Weather Service).

For construction of the about 6 ha sized catchment an 1-3 m thick base layer (aquiclude) of Tertiary clay was covered by a 2-3 m thick sandy, lignite- and pyrite-free Quaternary sediment serving as water storage layer (aquifer) (Gerwin et al. 2010, Kendzia et al. 2008). Quaternary material was taken from a depth of 20-30 m during lignite mining process and its texture is classified as sand to loamy sand with low contents of carbonate (Gerwin et al. 2009, 2010, Russell et al. 2010). Dumping of material and construction work with large machines (e.g., stackers and bulldozers) resulted in differently structured sections of Chicken Creek. Generally, the catchment area can be divided into four sections: i) an eastern part (ca. 1.8 ha), ii) a western part (ca. 1.6 ha), iii) a central trench (ca. 0.9 ha) separating the eastern from the western part and iv) a southern part (ca. 1.5 ha) with a pond at the lowest point (Fig. 1). Construction work was completed in 2005 (time zero, t_0). Analyses subsequent to catchment completion indicated slight differences in abiotic conditions (soil pH, conductivity, skeleton content (soil particle diameter >2 mm), proportions of sand, silt and clay, concentration of organic and inorganic carbon) between the eastern and the western part (Gerwin et al. 2010). In October 2007 four soil pits in combination with suction cups were installed at Chicken Creek for soil solution analyses. For detailed information on site construction and soil pit installation see Gerwin et al. (2010) and Schaaf et al. (2010), respectively.

2.2. Soil sampling

We took samples shortly after construction of Chicken Creek (t_0) and after an ecosystem development period of about ten years (t_{10}). For t_0 (no vegetation detectable) we assumed only very few biogenic siliceous structures homogenously distributed on the whole area of Chicken Creek, i.e., no section-specific distribution of BSi (BSi t_0 east ≈ BSi t_0 west ≈ BSi t_0

145 south) at the beginning of ecosystem development (Puppe et al. 2016). This is why we did
146 not sample all different sections of the catchment, but took soil samples in six field replicates
147 to quantify BSi pools at t_0. However, for t_{10} we hypothesized section-specific differences in
148 BSi pool quantities related to section-specific vegetation dynamics. To evaluate these
149 differences after a decade of ecosystem development and to cover the biggest possible BSi
150 accumulation in soil we focused on spots where Si accumulating plant species, i.e.,
151 *Calamagrostis epigejos* and *Phragmites australis* became dominant (Zaplata et al. 2010).
152 Thus we took samples in the eastern (*C. epigejos* dominant) and western (mainly *C. epigejos*
153 dominant, one spot with *P. australis*) and southern section (*P. australis* dominant) of Chicken
154 Creek.
155 For an accurate description of changes of abiotic soil conditions and related phytogenic Si in
156 every section we took soil and plant samples in eastern, western and southern sections at t_0
157 as well as t_{10}. Soil samples for the determination of soil properties and plant samples were
158 taken in five (western and southern section) and six (eastern section) field replicates at t_0
159 and t_{10} (Fig. 1). At every sampling point three undisturbed soil cores where taken with a core
160 cutter (diameter = 3.4 cm, depth = 5 cm) and transferred into plastic bags. Bulk densities
161 were calculated from dividing weight of dried (105°C) soil samples by corresponding volume.
162
163 *2.3. Determination of basic soil properties*
164 Soil samples were air dried and sieved and the fine earth fraction (<2 mm) was used for
165 laboratory analyses. Soil pH was measured based on the DIN ISO Method 10390 (1997) in
166 0.01 M $CaCl_2$ suspensions at a soil to solution ratio of 1:5 (*w/v*) after a 60 minute
167 equilibration period using a glass electrode. The total carbon content was analyzed by dry
168 combustion using an elemental analyzer (Vario EL, Elementar Analysensysteme, Hanau,

169 Germany). Carbonate ($CaCO_3$) was determined conductometrically using the Scheibler
170 apparatus (Schlichting et al. 1995). Organic carbon (C_{org}) was computed as the difference
171 between total carbon and carbonate carbon. Analyses of basic soil properties were
172 performed in two lab replicates per sample.
173
174 *2.3.1. Water Extractable Si (Si_{H2O})*
175 Water extractable Si was determined based on a method developed by Schachtschabel &
176 Heinemann (1967). Ten grams of dry soil (<2 mm) were weighed into 80 mL centrifuge tubes
177 and 50 mL distilled water added together with three drops of a 0.1% NaN_3-solution to
178 prevent microbial activity. Total extraction time was seven days in which tubes were shaken
179 by hand twice a day for twenty seconds. Mechanical (constant) shaking by using, e.g., a roll
180 mixer, was avoided to prevent abrasion of mineral particles colliding during shaking
181 (McKeague & Cline 1963). The solutions were centrifuged (4000 rpm, 20 min), filtrated (0.45
182 µm polyamide membrane filters) and Si was measured by ICP-OES, (ICP-iCAP 6300 DUO,
183 Thermo Fisher SCIENTIFIC GmbH). Analyses of water extractable Si were performed in two
184 lab replicates per sample.
185
186 *2.3.2. Tiron extractable Si (Si_{Tiron}), aluminum (Al_{Tiron}) and iron (Fe_{Tiron})*
187 The Tiron ($C_6H_4Na_2O_8S_2 \cdot H_2O$) extraction followed the method developed by Biermans &
188 Baert (1977), modified by Kodama & Ross (1991). It has been used to quantify amorphous
189 biogenic and pedogenic Si (Kendrick & Graham 2004), although a partial dissolution of
190 primary minerals is well known (Kodama & Ross 1991, Sauer et al. 2006). The extraction
191 solution was produced by dilution of 31.42 g Tiron with 800 mL of distilled water, followed
192 by addition of 100 mL sodium carbonate solution (5.3 g Na_2CO_3 + 100 mL distilled water)

193 under constant stirring. The final pH of 10.5 was reached by adding small volumes of a 4M
194 NaOH-solution. For the extraction 30 mg of dry soil were weighed into 80 mL centrifuge
195 tubes and a 30 mL aliquot of the Tiron solution was added. The tubes were then heated at
196 80°C in a water bath for 1h. The extracted solutions were centrifuged at 4000 rpm for 30
197 min, filtrated (0.45 µm polyamide membrane filters, Whatman NL 17) and Si, Al and Fe
198 measured by ICP-OES. Analyses of Tiron extractable Si, Al and Fe were performed in three
199 lab replicates per sample.
200
201 *2.4. Microscopical analyses of diatoms, sponge spicules and testate amoebae*
202 Fresh soil samples were homogenized by gentle turning of the plastic bags before air drying.
203 Afterwards 2 g of fresh soil were taken per sample and stored in 8 mL of formalin (4 %).
204 Subsequently, biogenic siliceous structures, i.e., diatom frustules, testate amoeba shells and
205 sponge spicules (Fig. 2A-D), were enumerated in soil suspensions (125 mg fresh mass (FM))
206 received from serial dilution (1000-125 mg soil in 8 mL of water each) using an inverted
207 microscope (OPTIKA XDS-2, objectives 20:1 and 40:1, equipped with a digital camera
208 OPTIKAM B9).
209
210 *2.5. Determination of phytoliths in soil samples*
211 10 g of dry soil material (<2 mm) were processed in four steps (adapted from Alexandre et
212 al. 1997). First organic matter was oxidized using H_2O_2 (30 Vol. %), HNO_3 (65 Vol. %) and
213 $HClO_4$ (70 Vol. %) at 80°C until reaction subsides. Secondly, carbonates and Fe oxides were
214 dissolved by boiling the sample in HCl (10 Vol. %) for 30 min. Thirdly, the <2 µm
215 granulometric fraction was removed by dispersion of the remaining solid phase of step 2
216 with 2 Vol. % sodium hexametaphosphate solution (6–12 h), centrifugation at 1000 rpm for

2–3 min, and subsequent decantation. Finally, the phytoliths were separated by shaking the remaining solid phase of step 3 with 30 mL of sodium polytungstate ($Na_6(H_2W_{12}O_{40})\cdot H_2O$) with a density of 2.3 g cm^{-3} and subsequent centrifugation at 3000 rpm for 10 min. Afterwards, the supernatant was carefully pipetted and filtered using 5 µm teflon filters. This step was repeated three times. The filter residue was washed with water, bulked, dried at 105°C, and weighted.

2.6. Quantification of biogenic Si pools

In general, biogenic siliceous structures consist of hydrated amorphous silica ($SiO_2\cdot nH_2O$). We assumed an average water content of about 10 % for these structures to avoid an overestimation of BSi pools (Mortlock & Froelich 1989).

Protophytic Si pools (represented by diatom frustules) were quantified by multiplication of Si contents per frustule with corresponding individual numbers (see Puppe et al. 2016). Protozoic Si pools (represented by testate amoebae) were quantified by multiplication of silica contents of diverse testate amoeba taxa (Aoki et al. 2007) with corresponding individual numbers (living plus dead individuals, for details see Puppe et al. 2014, 2015).

Zoogenic Si pools (represented by sponge spicule fragments) were calculated by multiplying volumes (µm^3) of the found spicule fragments with the density of biogenic Si (2.35 g cm^{-3}) and summing up the results. Volume measurements were conducted using a laser scanning microscope (Keyence VK-X110, magnification 200-2.000x) (details in Puppe et al. 2016). For laser scanning microscopy spicule fragments were taken from soil suspensions by micromanipulation, washed in dist. H_2O and placed on clean object slides. After air drying images of spicule fragments were acquired (software Keyence VK-H1XVD) and analyzed (software Keyence VK-H1XAD).

241 Phytogenic Si pools were estimated by multiplying the numbers of found phytoliths with
242 corresponding mean volumes (μm^3) of phytoliths, multiplying these results with the density
243 of biogenic Si (2.35 g cm^{-3}) and summing up the results. Volume measurements with the
244 laser scanning microscope of 30 typical elongate (Fig. 2E) and 30 typical bilobate phytoliths
245 (Fig. 2F) resulted in mean volumes of 3765 μm^3 and 707 μm^3, respectively. For laser scanning
246 microscopy extracted phytoliths were placed on clean object slides and images were
247 acquired and analyzed analogous to sponge spicules. For bilobate phytoliths we measured
248 the upper half per phytolith and doubled the result to obtain the corresponding total
249 volume, thus we assumed bilobate phytoliths to be symmetric. We assumed phytoliths to
250 consist of 95 % SiO_2 and 5 % other elements, i.e., carbon (Song et al. 2012) and other
251 elements like iron, aluminum or calcium (Buján 2013).
252 BSi pools (mg m^{-2}) were calculated considering bulk density (g cm^{-3}), thickness (5 cm) and –
253 for protistic and zoogenic Si pools – water content (% of fresh mass) per soil sample. Silica
254 (M = 60.08 g mol^{-1}) pools were converted to Si (M = 28.085 g mol^{-1}) pools by multiplication
255 with 28/60 (details in Puppe et al. 2014, 2015, 2016).
256
257 *2.7. Plant analyses*
258 Plant (aboveground plant material only) and litter samples of *C. epigejos* and *P. australis*
259 were collected in the summer of 2015. The collected plant material was washed with
260 distilled water to remove adhering soil minerals and oven-dried at 45°C for 48 hours.
261
262 *2.7.1. Total Si content in plant materials*
263 Plant samples were milled using a knife mill (Grindomix GM 200, Retsch) in two steps: 4.000
264 rpm for 1 min and then 10.000 rpm for 3 min. Sample aliquots of approximately 100 mg

were digested under pressure in PFA digestion vessels using a mixture of 4 mL distilled water, 5 mL nitric acid (65 %), and 1 mL hydrofluoric acid (40 %) at 190°C using a microwave digestion system (Mars 6, CEM). A second digestion step was used to neutralize the hydrofluoric acid with 10 mL of a 4 %-boric acid solution at 150°C. Silicon was measured by ICP-OES (ICP-iCAP 6300 Duo, Thermo Fisher Scientific GmbH) with an internal standard. To avoid contamination, plastic equipment was used during the complete procedure. Analyses of total Si content were performed in three lab replicates per sample.

2.7.2. Determination of phytoliths in plants and litter

Plant material was washed with distilled water and oven-dried at 45°C for 48 hours. Removal of organic matter was conducted by burning the samples in a muffle furnace at 450°C for 12 hours. Next, the material was subject to additional oxidation using 30 % H_2O_2 for 12 hours. The obtained material was filtered through a teflon filter with a mesh size of 5 µm. The isolated phytoliths and siliceous cast (>5 µm) were subject to analysis via polarized light microscopy (Nikon ECLIPSE LV100 microscope) for full characteristics. We used laser scanning microscopy for measurements of the surface-area (μm^2) of the 30 typical bilobate and 30 typical elongated phytoliths used for volume measurements (see 2.6) and calculated corresponding surface-area-to-volume ratios (A/V ratios) as an indicator for the resistibility of these siliceous structures against dissolution. Higher A/V ratios indicate a bigger surface-area available for dissolution processes.

2.8. Statistical analyses

Correlations were analyzed using Spearman's rank correlation (r_s). Significances in two-sample (n = 2) cases were verified with the Mann-Whitney U-test. For *k*-sample (n > 2) cases

289 the Kruskal-Wallis analysis of variance (ANOVA) was used followed by pairwise multiple
290 comparisons (Dunn's post hoc test). Statistical analyses were performed using software
291 package SPSS Statistics (version 19.0.0.1, IBM Corp.).
292
293 **3. Results**
294 *3.1. Basic soil parameters*
295 Soils at the initial state (t_0) showed in the upper 5 cm organic carbon contents (C_{org}) between
296 1.1 g kg^{-1} and 4.4 g kg^{-1} in the western section, 0.8 g kg^{-1} and 1.8 g kg^{-1} in the eastern section
297 and 0.2 g kg^{-1} and 3.3 g kg^{-1} in the southern section. This corresponded to mean carbon
298 stocks of 237 g m^{-2} (west), 123 g m^{-2} (east) and 160 g m^{-2} (south, Table 1). After 10 years (t_{10})
299 of ecosystem development the C_{org} stocks increased up to a factor of 3 (396-556 g m^{-2} in the
300 upper 5 cm) compared to corresponding values at t_0. This resulted in a surprisingly high
301 mean annual CO_2-C sequestration rate of 27-32 g m^{-2} (upper 5 cm). Hereby the largest C_{org}
302 stock changes were found in the western section of the area followed by the eastern section
303 and the southern section (Table 1).
304 The carbonate contents ($CaCO_3$) at t_0 varied between means of 1.0 g kg^{-1} (west), 0.9 g kg^{-1}
305 (east) and 1.8 g kg^{-1} (south). The corresponding stocks were 88 g m^{-2} (west), 91 g m^{-2} (east)
306 and 174 g m^{-2} (south, Table 1). The carbonate pools in the western and eastern section were
307 very similar, while the high carbonate values in the southern section were due to the original
308 soil properties. At t_{10} the distribution of carbonate was as follows: in the western section
309 there was an increase of about 17 % (from 88 g m^{-2} to 101 g m^{-2}), in the eastern part a
310 distinct decrease of about 67 % (from 91 g m^{-2} to 30 g m^{-2}) was detected and in the southern
311 section again a decrease of about 28 % (from 174 g m^{-2} to 126 g m^{-2}) was identified.

312 At t_0 the pH values of the soils showed a range between 7.9 and 8.3 (Table 1) with relatively
313 low variation between the different sections. After 10 years the pH values decreased to 7.1-
314 7.4 in all sections.

315

316 *3.2. Water and Tiron extractions*

317 The mean water soluble Si (Si_{H2O}) contents in the upper 5 cm showed low variation between
318 the different sections at t_0: 7.3 x 10^{-3} g kg^{-1} (west), 7.2 x 10^{-3} g kg^{-1} (east) and 8.6 x 10^{-3} g kg^{-1}
319 (south). The corresponding stock values were 0.7 g m^{-2} (west), 0.87 g m^{-2} (east) and 0.84 g m^{-2}
320 (south) for all sections at t_0 (Table 1). After 10 years (t_{10}) an overall significant increase of
321 Si_{H2O} in each of the different sections compared to t_0 was found. The corresponding stock
322 values were 1.7 g m^{-2} (west), 1.5 g m^{-2} (east) and 2.2 g m^{-2} (south, Table 1).
323 At t_0 the mean Tiron extractable Si contents in the upper 5 cm varied between 5.5 g kg^{-1}
324 (west), 5.2 g kg^{-1} (east) and 4.1 g kg^{-1} (south). The related stock values were 524 g m^{-2} (west),
325 503 g m^{-2} (east) and 399 g m^{-2} (south, Table 1). After 10 years (t_{10}) the Tiron extractable Si
326 content showed a slight increase in the western section to 6.5 g kg^{-1} (552 g m^{-2}), while the
327 concentration in the eastern section decreased significantly to 2.6 g kg^{-1} (196 g m^{-2}, Table 1).
328 In the southern section only a slight decrease to 3.8 g kg^{-1} (317 g m^{-2}) was found. The Al and
329 Fe extractable Tiron contents followed the distribution of the Si concentrations with one
330 exception in the western section, where contrary to Si the Al and the Fe contents slightly
331 increased at t_{10} (Table 1). Si/Al ratios ranged between 1.6 and 2.2 at Chicken Creek. Tiron
332 extractable Si and Al fractions as well as Tiron extractable Al and Fe fractions were strongly
333 correlated (Table 2).

334

335

Biogeosciences Discuss., https://doi.org/10.5194/bg-2017-177
Manuscript under review for journal Biogeosciences
Discussion started: 20 June 2017

336 *3.3. Biogenic Si pools in soils*

337 In general, total biogenic Si pools increased in every section after ten years of ecosystem
338 development with statistically significant differences between t_0 (11.6 ± 6.5 mg Si m^{-2}) and
339 the southern section at t_{10} (96.0 ± 87.2 mg Si m^{-2}) (Fig. 3). Total BSi showed strong positive
340 and statistically significant correlations to water soluble Si (Table 2). Phytogenic (phytoliths
341 >5 µm) Si pools ranged from 0-18 mg m^{-2} (mean: 6.6 mg m^{-2}) at t_o and significantly increased
342 to means of 20.7 mg m^{-2} (range: 7-52 mg m^{-2}) and 12.9 mg m^{-2} (range: 14-15 mg m^{-2}) at the
343 eastern and southern section during 10 years, respectively (Fig. 4A). Protophytic Si pools
344 (diatom frustules) ranged from 0-7 mg m^{-2} (mean: 2.6 mg m^{-2}) at t_0 and increased up to a
345 mean of 47.4 mg m^{-2} (range: 0.1-162 mg m^{-2}) at t_{10} (southern section) (Fig. 4B). At t_0 no
346 sponge spicules were found with one exception representing an extreme value (12.7 mg m^{-2}).
347 After one decade of ecosystem development zoogenic Si pools increased to a maximum
348 of 46 mg m^{-2} at the southern section (t_{10}) (Fig. 4C). Protozoic Si pools were zero at t_0 with
349 one exception representing an extreme value (1.8 mg m^{-2}) and significantly increased to 4.6
350 mg m^{-2} (range: 1-11 mg m^{-2}) and 11.5 mg m^{-2} (range: 2-36 mg m^{-2}) in the eastern and the
351 southern section at t_{10}, respectively (Fig. 4D).
352 At t_0 most BSi (>50 %) is represented by phytoliths >5 µm followed by diatom frustules,
353 sponge spicules and testate amoeba shells (Fig. 5). After ten years of ecosystem
354 development the proportion of the different BSi pools to total BSi changed. While the
355 proportion of protozoic Si pools increased in all sections at t_{10}, the other BSi pools showed
356 more variable changes over time. The proportion of phytogenic Si pools either increased
357 (western section) or decreased (eastern and southern sections). In contrast, the proportion
358 of protophytic Si pools decreased at the western section and increased in the eastern and

Biogeosciences Discuss., https://doi.org/10.5194/bg-2017-177
Manuscript under review for journal Biogeosciences
Discussion started: 20 June 2017

359 southern sections. The proportion of zoogenic Si pools decreased in the western and eastern
360 sections, but increased slightly in the southern section at t_{10}.
361
362 *3.4. Phytoliths and total Si content in plant materials*
363 The total content of Si was determined for two Si accumulating plant species *Calamagrostis*
364 *epigejos* and *Phragmites australis* dominating distinct catchment sections. For *C. epigejos*
365 the mean total content of Si was 2.25 % (range: 1.8-3.1 %), whereas for *P. australis* a mean
366 total Si content of 2.70 % (range: 2.0-3.2 %) was determined (Fig. 6A, B). For litter we found
367 mean total Si contents of 3.1 % (range: 2.8-3.3 %) and 2.9 % (range: 1.7-3.2 %) for *C. epigejos*
368 and *P. australis*, respectively.
369 Phytoliths >5 µm were also isolated from both plants; for *C. epigejos* the mean phytolith
370 content was 0.37 % (range: 0.31-0.46 %), whereas for *P. australis* a mean phytolith content
371 of 0.43 % (range: 0.37-0.50 %) was determined (Fig. 6A, B), i.e., related to the total Si
372 content of plants 16.4 % and 15.9 % of phytogenic Si were represented by phytoliths >5 µm
373 in *C. epigejos* and *P. australis*, respectively. Thus, small-scale (<5 µm) and fragile (siliceous
374 structures mostly thinner than 5 µm, but up to several hundred micrometers long, Fig. 7)
375 phytogenic Si represented 83.6 % and 84.1 % of total phytogenic Si in *C. epigejos* and *P.*
376 *australis*, respectively. Mean phytolith contents in plant litter were 0.47 % (range: 0.35-
377 0.70 %) and 0.51 % (range: 0.41-0.59 %) for *C. epigejos* and *P. australis*, respectively.
378 Surface-areas of 30 typical bilobate and 30 typical elongate phytoliths were in a range of 216
379 μm^2 to 3,730 μm^2 and 2,302 μm^2 to 22,203 μm^2, respectively (Table 3). The corresponding
380 volumes of bilobate and elongate phytoliths were in a range of 36 μm^3 to 2,046 μm^3 and 390
381 μm^3 to 14,649 μm^3, respectively. Surface-to-volume ratios of bilobate and elongate

phytoliths were in a range of 0.7 to 9.8 and 0.6 to 5.9 with means of 2.8 and 2.6, respectively.

3.5. BSi and Si fractions under Calamagrostis epigejos *and* Phragmites australis

Water soluble Si fractions increased by 99 % and 163 %, total BSi by 281 % and 660 % after ten years of ecosystem development in soils under *C. epigejos* and *P. australis*, respectively. In contrast, Si_{Tiron} decreased by 42 % and 1.4 % from t_0 to t_{10} in soils under *C. epigejos* and *P. australis*, respectively. If we assume mean dry biomasses of 115 g m^{-2} and 186 g m^{-2} for *C. epigejos* and *P. australis* (M. Wehrhan, pers. comm., 2017) about 2.6 g Si m^{-2} and 5.0 g Si m^{-2} are stored in the aboveground biomass at Chicken Creek, respectively. For litter of *C. epigejos* and *P. australis* (mean dry biomasses of 59 g m^{-2} and 94 g m^{-2}, M. Wehrhan, pers. comm., 2017) we calculated corresponding pools of about 1.8 g Si m^{-2} and 2.7 g Si m^{-2}, respectively.

4. Discussion

4.1. Drivers of short-term changes of water soluble Si at Chicken Creek

In general, weathering of silicates represents the ultimate source of $Si(OH)_4$ in terrestrial biogeosystems in the long term (Berner 2003). In this context, the long-term accumulation of BSi can influence the total amorphous (Tiron extractable) Si as it is known from forested catchments or old chronosequence soils (Conley et al. 2008, Kendrick & Graham 2004, Saccone et al. 2008). Contrary, short-term changes of BSi pools likely do not influence Tiron extractable Si in initial soils (total BSi represents only 0.002-0.03 % of Tiron extractable Si at Chicken Creek). Thus, the major proportion of Tiron extractable Si at Chicken Creek seems to be of pedogenic origin (e.g., Si included in Al/Fe oxides/hydroxides). This is supported by

406 relatively low Si/Al ratios (<5) indicating a minerogenic origin of Tiron extractable Si instead
407 of BSi as a source of Si_{Tiron} (Bartoli & Wilding 1980). We further exclude changes of Tiron
408 extractable Si as the main driver of water soluble Si at Chicken Creek in the short term,
409 because i) Si_{Tiron} and Si_{H2O} showed no statistical relationship at all and ii) a significant change
410 of the Tiron extractable Si fraction only occurred only in the eastern section, whereas in the
411 western and southern section Si_{Tiron} did not change significantly over time. We assume that
412 these changes of Si_{Tiron} in the eastern section are related to abiotic conditions (soil pH,
413 conductivity, skeleton content, proportions of sand, silt and clay, concentration of organic
414 and inorganic carbon), which were slightly different to the conditions of the western section
415 already at t_0 (Gerwin et al. 2010).
416 Our results indicate a strong relationship between water soluble Si and total BSi. In this
417 context, two different causal chains can be discussed: Either SiO_2-synthesizing organisms are
418 drivers of the amount of $Si(OH)_4$ in the soil or – *vice versa* – the amount of water soluble Si in
419 the soils is the main driver of SiO_2-synthesizing organisms as biosilicification is limited by
420 $Si(OH)_4$. Laboratory studies, for example, revealed that SiO_2-synthesizing organisms, i.e.,
421 testate amoebae, can deplete the amount of $Si(OH)_4$ in culture media due to biosilicification
422 (Aoki et al. 2007, Wanner et al. 2016). However, Wanner et al. (2016) also showed that
423 culture growth of SiO_2-synthesizing testate amoebae was dependent on Si concentration in
424 the culture media. Furthermore, *in situ* analyses showed that marine diatom blooms can
425 deplete $Si(OH)_4$ concentrations in the oceans (Hildebrand 2008). In forested biogeosystems
426 Puppe et al. (2015) found high individual numbers of SiO_2-synthesizing testate amoebae at
427 study sites with low amounts of $Si(OH)_4$ and *vice versa*. However, it is unlikely that testate
428 amoebae depleted amounts of $Si(OH)_4$ at these sites, because corresponding protozoic Si
429 pools are relatively small compared to phytogenic ones (Puppe et al. 2015, Sommer et al.

2013). Regarding vegetation and corresponding phytogenic Si pools their influence on the amount of $Si(OH)_4$ in soils has been shown in several studies (e.g., Bartoli 1983, Farmer et al. 2005, Sommer et al. 2013). On the other hand, phytolith production is probably more influenced by the phylogenetic position of a plant than by environmental factors like temperature or Si availability (Hodson et al. 2005, Cooke & Leishman 2012).

From our results and the discussion above we conclude short-term changes of water soluble Si to be mainly driven by BSi. However, total BSi represents only small proportions of water soluble Si at t_0 (<2 %) and t_{10} (<4.5 %). From this result the question arises, where does the major part of the increase in water soluble Si at Chicken Creek come from? We will discuss this question in the subsection (4.2.) below.

4.2. Sources of water soluble Si at Chicken Creek

From further results of BSi analyses in forested biogeosystems, we assumed the phytogenic Si pool to be the most prominent in size. In this context, results of Sommer et al. (2013) and Puppe et al. (2015) showed that phytogenic Si pools in soils of forested biogeosystems were up to several hundred times larger than protozoic Si pools. However, phytogenic Si pools in soils are surprisingly small compared to other BSi pools at Chicken Creek. Our findings can be attributed to at least two reasons. Firstly, phytogenic Si is stored in a developing organic litter layer where it is temporarily protected against dissolution and secondly, the used methods were not able to accurately quantify the total phytogenic Si pool, but only the larger part (>5 μm).

Total Si and phytolith contents of litter samples at Chicken Creek did not differentiate from total Si and phytolith contents of plants. This fact indicates that litter decomposition and related Si release into the subjacent soil are relatively slow processes and we interpret our

findings as a hint for a developing compartment of dead plant tissue above the mineral soil surface. Esperschütz et al. (2013) showed in a field experiment in initial soils near Chicken Creek that after 30 weeks only 50 % of the litter of *C. epigejos* were degraded, whereby degradation rates were highest in the first four weeks. Estimations of biomasses of *C. epigejos* and *P. australis* at Chicken Creek via remote sensing with an unmanned aerial system showed that the relation between phytogenic Si pools plant biomass and litter biomass is almost the same for both plant species (factor about 1.5, based on the total area of Chicken Creek), i.e., Si in the plants was about one third higher than in litter (M. Wehrhan, pers. comm., 2017, manuscript in preparation). At the sampling points about 1.8 g Si m^{-2} and 2.7 g Si m^{-2} were stored in the litter of *C. epigejos* and *P. australis*, respectively, which is in the range of published data for annual Si input through litterfall in a short grass steppe (2.2-2.6 g Si m^{-2} per year, Blecker et al. 2006).

Altogether, these results clearly underline our interpretation of a developing organic layer where litter accumulates and phytogenic Si is temporarily stored and protected against dissolution, thus Si release is delayed biologically controlled as it can be observed at forested biogeosystems (Sommer et al. 2013). The Si pools in the aboveground biomass of *C. epigejos* (2.6 g Si m^{-2}) and *P. australis* (5.0 g Si m^{-2}) at Chicken Creek are comparable to reported values of Great Plains grasslands (2.2-6.7 g Si m^{-2} in the aboveground biomass) (Blecker et al. 2006) and reach about 30 % (*C. epigejos*) or 59 % (*P. australis*) of published data for a beech forest (8.5 g Si m^{-2} in the aboveground biomass of *Fagus sylvatica* trees) in northern Brandenburg, Germany (Sommer et al. 2013), after (only) ten years of ecosystem development.

Regarding methodological shortcomings there are several points to be discussed. Wilding & Drees (1971), for example, showed that about 72 % of leaf phytoliths of American beech

(*Fagus grandifolia*) are smaller than 5 µm. This is in accordance with our findings. Phytoliths <5 µm only amounted to about 16 % of total Si contents of plant materials of *C. epigejos* and *P. australis*, thus about 84 % of phytogenic Si are not quantified by the used phytolith extraction. Watteau & Villemin (2001) found even smaller (5-80 nm) spherical grains of pure silica in leaf residues in topsoil samples of a forested biogeosystem. In addition, silica depositions can be found in intercellular spaces or in an extracellular (cuticular) layer (Sangster et al. 2001), whereat no recognizable phytoliths are formed. These structures might be too fragile for preservation in soils and are likely lost in the used phytolith extraction procedure due to dissolution. Meunier et al. (2017) analyzed different phytolith morphotypes, e.g, silica bodies originating from cells of the upper epidermis, silica casts of trichomes or parenchyma/collenchyma cells, of durum wheat plant shoots. They found fragile sub-cuticular silica plates (2-4 µm thick, up to several hundred micrometers long and wide) to be the second most common phytolith morphotype. This is corroborated by our own findings as the biggest part (about 84 %) of total plant Si is represented by small-scale (<5 µm) and fragile phytogenic Si in *C. epigejos* and *P. australis*. If we assume that total Si contents of plants at Chicken Creek are one-to-one reflected by phytogenic Si pools in soils we can easily calculate these small-scale and fragile pools resulting in about 130 mg m^{-2} and 100 mg m^{-2} (84 % of total, i.e., 156 mg m^{-2} and 119 mg m^{-2}, phytogenic Si each) under *C. epigejos* and *P. australis*, respectively. These calculated phytogenic Si pools are about 13 (diatom frustules), 38 (testate amoeba shells) and 45 (sponge spicules) or 3 (diatom frustules) and 10 (testate amoeba shells, sponge spicules) times bigger than the other BSi pools at *C. epigejos* and *P. australis* sampling points, respectively. If we further assume an input of this phytogenic Si for at least seven years (Zaplata et al. 2010) phytogenic Si might be the main driver of short-term changes of water soluble Si at Chicken Creek. This is

supported by relatively high surface-to-volume ratios of bilobate and elongate phytoliths. These ratios are about three times higher compared to ratios of other biogenic siliceous structures, i.e., testate amoeba shells, diatom frustules and sponge spicules.

In addition, Si pools represented by single siliceous platelets of testate amoeba shells have to be considered as well as these platelets can be frequently found in freshwater sediments, for example (Douglas & Smol 1987, Pienitz et al. 1995). Unfortunately, there is no information on the quantity of such platelet pools in soils available, but it can be assumed that these platelets can be frequently found in soils as they are used by some testate amoeba genera (e.g., *Schoenbornia*, *Heleopera*) for shell construction (Meisterfeld 2002, Schönborn et al. 1987). In general, it can be assumed that phytogenic Si structures <5 µm and single testate amoeba platelets (about 3-12 µm in diameter, Douglas & Smol 1987) are highly reactive due to their relatively high surface/volume ratios. However, to the best of our knowledge there is no publication available dealing with corresponding physicochemical analyses or dissolution kinetics of these siliceous structures. In general, experiments with phytoliths (>5 µm) showed that surface-areas and related dissolution susceptibilities are, for example, age-related due to changes in specific surface areas and the presence of organic matter bound to the surface of phytoliths (Fraysse et al. 2006, 2009).

5. Conclusions

Decadal changes of water soluble Si at Chicken Creek are mainly driven by BSi, thus Si cycling is biologically controlled already at the very beginning of ecosystem development. In this context, especially phytogenic Si plays a prominent role. However, a developing organic layer (L horizon) at the soil surface temporarily protects phytogenic Si against dissolution, because phytogenic Si is still incorporated in plant structural elements (tissues). In consequence a

526 delaying biogenic Si pool is built up and Si release into the soil is retarded. Furthermore,
527 established phytolith extraction methods alone are not suitable to quantify total phytogenic
528 Si pools as phytoliths >5 µm seem to be only a minor part of this pool (about 16 % in the
529 current study). In general, information on small-scale (<5 µm) and fragile phytogenic Si
530 structures are urgently needed as they seem to represent the biggest and most reactive Si
531 pool in soils, thus the most important driver of Si cycling in terrestrial biogeosystems. Future
532 work should focus on i) the quantification of this pool, ii) physicochemical analyses of its
533 components, and (iii) their dissolution kinetics in lab experiments. The combination of
534 modern microscopical (SEM-EDX, laser scanning microscopy) (this study, Puppe et al. 2016,
535 Sommer et al. 2013) and spectroscopical (FTIR and micro-FTIR spectroscopy) (Liu et al. 2013,
536 Loucaides et al. 2010, Rosén et al. 2010) methods might introduce new insights in this field.
537
538
539
540 **Acknowledgements**
541 This study has been financed by the DFG project 'Spatiotemporal dynamics of biogenic Si
542 pools in initial soils and their relevance for desilication' (SO 302/7-1). Many thanks to
543 Christian Buhtz and Reneé Ende for their excellent laboratory support. We would like to
544 thank the members of the 'Chicken Creek project' at BTU Cottbus-Senftenberg for providing
545 soil samples from 2005 and organizational support. Vattenfall Europe Mining AG provided
546 the research site. This study is a contribution to the Transregional Collaborative Research
547 Centre 38 (SFB/TRR 38) financially supported by the German Research Council (DFG, Bonn)
548 and the Brandenburg Ministry of Science, Research and Culture (MWFK, Potsdam).
549

References

Alexandre, A., Meunier, J. D., Colin, F., Koud, J. M., 1997. Plant impact on the biogeochemical cycle of silicon and related weathering processes. *Geochimica et Cosmochimica Acta* 61, 677-682.

Aoki, Y., Hoshino, M., Matsubara, T., 2007. Silica and testate amoebae in a soil under pine–oak forest. *Geoderma* 142, 29-35.

Barão, L., Clymans, W., Vandevenne, F., Meire, P., Conley, D.J., Struyf, E., 2014. Pedogenic and biogenic alkaline-extracted silicon distributions along a temperate land-use gradient. *Eur. J. Soil Sci.* 65, 693-705.

Bartoli, F., 1983. The biogeochemical cycle of silicon in two temperate forest ecosystems. Environ. *Biogeochem. Ecol. Bull.* 35, 469-476.

Bartoli, F. & L. P. Wilding, 1980. Dissolution of biogenic opal as a function of its physical and chemical properties. *Soil Science Society of America Journal* 44, 873-878.

Berner, R. A., 2003. The long-term carbon cycle, fossil fuels and atmospheric composition. *Nature* 426, 323-326.

Biermans, V., Baert, L., 1977. Selective extraction of the amorphous Al, Fe and Si oxides using an alkaline Tiron solution. *Clay Miner.*, 12, 127-135.

Blecker, S. W., McCulley, R. L., Chadwick, O. A. & Kelly, E. F., 2006. Biologic cycling of silica across a grassland bioclimosequence. *Global Biogeochemical Cycles* 20, GB3023.

Buján, E., 2013. Elemental composition of phytoliths in modern plants (Ericaceae). *Quaternary International* 287, 114-120.

571 Clarke, J., 2003. The occurrence and significance of biogenic opal in the regolith. *Earth-Sci.*
572 *Rev.* 60, 175-194.

573 Clymans, W., Struyf, E., Govers, G., Vandevenne, F., Conley, D.J., 2011. Anthropogenic impact
574 on amorphous silica pools in temperate soils. *Biogeosciences* 8, 2281-2293.

575 Conley, D. J., G. E. Likens, D. C. Buso, L. Saccone, S. W. Bailey & C. E. Johnson, 2008.
576 Deforestation causes increased dissolved silicate losses in the Hubbard Brook Experimental
577 Forest. *Global Change Biology* 14, 2548-2554.

578 Cooke, J. & Leishman, M. R., 2012. Tradeoffs between foliar silicon and carbon-based
579 defences: evidence from vegetation communities of contrasting soil types. *Oikos* 121, 2052-
580 2060.

581 Creevy, A.L., Fisher, J., Puppe, D., Wilkinson, D.M., 2016. Protist diversity on a nature reserve
582 in NW England – with particular reference to their role in soil biogenic silicon pools.
583 *Pedobiologia* 59, 51-59.

584 DIN ISO 1039, 1997. Bodenbeschaffenheit: Bestimmung des pH-Wertes. Deutsches Institut
585 für Normung, Beuth, Berlin.

586 Douglas, M.S. & J.P. Smol, 1987. Siliceous protozoan plates in lake sediments. *Hydrobiologia*
587 154, 13-23.

588 Dürr, H.H., Meybeck, M., Hartmann, J., Laruelle, G.G., Roubeix, V., 2011. Global spatial
589 distribution of natural riverine silica inputs to the coastal zone. *Biogeosciences* 8, 597-620.

590 Ehrlich, H., Demadis, K.D., Pokrovsky, O.S., Koutsoukos, P.G., 2010. Modern views on
591 desilicification: biosilica and abiotic silica dissolution in natural and artificial environments.
592 *Chem. Rev.* 110, 4656-4689.

593 Epstein, E., 2009. Silicon: its manifold roles in plants. *Annals of Applied Biology* 155, 155-160.

594 Esperschütz, J., Zimmermann, C., Dümig, A., Welzl, G., Buegger, F., Elmer, M., Munch, J. C.,
595 Schloter, M., 2013. Dynamics of microbial communities during decomposition of litter from
596 pioneering plants in initial soil ecosystems. *Biogeosciences* 10, 5115-5124.

597 Farmer, V. C., Delbos, E., Miller, J. D., 2005. The role of phytolith formation and dissolution in
598 controlling concentrations of silica in soil solutions and streams. *Geoderma* 127, 71-79.

599 Fraysse, F., Pokrovsky, O. S., Schott, J., Meunier, J. D., 2006. Surface properties, solubility and
600 dissolution kinetics of bamboo phytoliths. *Geochimica et Cosmochimica Acta* 70, 1939-1951.

601 Fraysse, F., Pokrovsky, O. S., Schott, J., Meunier, J. D., 2009. Surface chemistry and reactivity
602 of plant phytoliths in aqueous solutions. *Chemical Geology* 258, 197-206.

603 Frings, P. J., Clymans, W., Jeppesen, E., Lauridsen, T. L., Struyf, E., Conley, D. J., 2014. Lack of
604 steady-state in the global biogeochemical Si cycle: emerging evidence from lake Si
605 sequestration. *Biogeochemistry* 117, 255-277.

606 Gerwin, W., Schaaf, W., Biemelt, D., Fischer, A., Winter, S., Hüttl, R.F., 2009. The artificial
607 catchment 'Chicken Creek' (Lusatia, Germany) – A landscape laboratory for interdisciplinary
608 studies of initial ecosystem development. *Ecol. Eng.* 35, 1786-1796.

609 Gerwin, W., Schaaf, W., Biemelt, D., Elmer, M., Maurer, T., Schneider, A., 2010. The Artificial
610 catchment 'Hühnerwasser' (Chicken Creek): construction and initial properties. Ecosystem
611 Development 1 (edited by Hüttl, R.F., Schaaf, W., Biemelt, D., Gerwin, W), Brandenburg
612 University of Technology Cottbus-Senftenberg, Germany.

613 Hildebrand, M., 2008. Diatoms, biomineralization processes, and genomics. *Chemical*
614 *Reviews* 108, 4855-4874.

615 Hodson, M. J., White, P. J., Mead, A., Broadley, M. R., 2005. Phylogenetic variation in the
616 silicon composition of plants. *Annals of Botany* 96, 1027-1046.

617 Keller, C., Guntzer, F., Barboni, D., Labreuche, J., Meunier, J.D., 2012. Impact of agriculture
618 on the Si biogeochemical cycle: input from phytolith studies. *C. R. Geosci.* 344, 739-746.

619 Kendrick, K. J., Graham, R.C., 2004. Pedogenic silica accumulation in chronosequence soils,
620 Southern California. *Soil Sci. Soc. Am. J.* 68, 1295-1303.

621 Kodama, H., Ross, G.J., 1991. Tiron dissolution method used to remove and characterize
622 inorganic components in soils. *Soil Sci. Soc. Am. J.* 55, 1180-1187.

623 Kendzia, G., Reißmann, R., Neumann, T., 2008. Targeted development of wetland habitats
624 for nature conservation fed by natural inflow in the post-mining landscape of Lusatia. *World*
625 *Min.* 60, 88-95.

626 Liu, X., S.M. Colman, E.T. Brown, E.C. Minor & H. Li, 2013. Estimation of carbonate, total
627 organic carbon, and biogenic silica content by FTIR and XRF techniques in lacustrine
628 sediments. *Journal of Paleolimnology* 50, 387-398.

629 Loucaides, S., T. Behrends & P. Van Cappellen, 2010. Reactivity of biogenic silica: Surface
630 versus bulk charge density. *Geochimica et Cosmochimica Acta* 74, 517-530.

631 Ma, J. F. & N. Yamaji, 2008. Functions and transport of silicon in plants. *Cellular and*
632 *Molecular Life Sciences* 65, 3049-3057.

633 McKeague, J.A., Cline, M.G., 1963. Silica in soil solutions I. The form and concentration of
634 dissolved silica in aqueous extracts of some soils. *Can. J. Soil Sci.* 43, 70-82.

635 Meisterfeld, R. (2002). Order Arcellinida Kent, 1880. The illustrated guide to the Protozoa
636 (ed. by J. J. Lee, G. F. Leedale & P. Bradbury), pp. 827-860. Society of Protozoologists,
637 Lawrence, KS, USA.

638 Meunier, J.D., Colin, F., Alarcon, C., 1999. Biogenic silica storage in soils. *Geology* 27, 835-
639 838.

640 Meunier, J. D., Barboni, D., Anwar-ul-Haq, M., Levard, C., Chaurand, P., Vidal, V., Grauby, O.,
641 Huc, R., Laffont-Schwob, I., Rabier, J., Keller, C., 2017. Effect of phytoliths for mitigating
642 water stress in durum wheat. *New Phytologist*, doi: 10.1111/nph.14554.

643 Mortlock, R.A., Froelich, P.N., 1989. A simple method for the rapid determination of biogenic
644 opal in pelagic marine sediments. *Deep-Sea Res.* 36, 1415-1426.

645 Pienitz, R., M.S. Douglas, J.P. Smol, P. Huttunen & J. Meriläinen, 1995. Diatom, chrysophyte
646 and protozoan distributions along a latitudinal transect in Fennoscandia. *Ecography* 18, 429-
647 439.

648 Puppe, D., Kaczorek, D., Wanner, M., Sommer, M., 2014. Dynamics and drivers of the
649 protozoic Si pool along a 10-year chronosequence of initial ecosystem states. *Ecol. Eng.* 70,
650 477-482.

651 Puppe, D., Ehrmann, O., Kaczorek, D., Wanner, M., Sommer, M., 2015. The protozoic Si pool
652 in temperate forest ecosystems – Quantification, abiotic controls and interactions with
653 earthworms. *Geoderma* 243-244, 196-204.

654 Puppe, D., Höhn, A., Kaczorek, D., Wanner, M., Sommer, M., 2016. As Time Goes By –
655 Spatiotemporal Changes of Biogenic Si Pools in Initial Soils of an Artificial Catchment in NE
656 Germany. *Appl. Soil Ecol.* 105, 9-16.

657 Rosén, P., H. Vogel, L. Cunningham, N. Reuss, D.J. Conley & P. Persson, 2010. Fourier
658 transform infrared spectroscopy, a new method for rapid determination of total organic and
659 inorganic carbon and biogenic silica concentration in lake sediments. *Journal of*
660 *Paleolimnology* 43, 247-259.

661 Russell, D.J., Hohberg, K., Elmer, M., 2010. Primary colonisation of newly formed soils by
662 actinedid mites. *Soil Org.* 82, 237-251.

663 Saccone, L., D. J. Conley, G. E. Likens, S. W. Bailey, D. C. Buso & C. E. Johnson, 2008. Factors
664 that control the range and variability of amorphous silica in soils in the Hubbard Brook
665 Experimental Forest. *Soil Science Society of America Journal* 72, 1637-1644.

666 Schönborn, W., W. Petz, M. Wanner & W. Foissner (1987). Observations on the Morphology
667 and Ecology of the Soil-Inhabiting Testate Amoeba *Schoenbornia humicola* (Schönborn,
668 1964) Decloitre, 1964 (Protozoa, Rhizopoda). *Archiv für Protistenkunde* 134, 315-330.

669 Sangster, A. G., Hodson, M. J. & H. J. Tubb (2001). Silicon deposition in higher plants, pp. 85-
670 113, in: Datnoff, L. E., Snyder, G. H. & G. H. Korndörfer (eds.). Silicon in agriculture (Vol. 8).
671 Elsevier, Amsterdam, The Netherlands.

672 Sauer, D., Saccone, L., Conley, D.J., Herrmann, L., Sommer, M., 2006. Review of
673 methodologies for extracting plant-available and amorphous Si from soils and aquatic
674 sediments. *Biogeochem.* 80, 89-108.

675 Schaaf, W., Biemelt, D., Hüttl, R.F., 2010. Initial development of the artificial catchment
676 'Chicken Creek' – monitoring program and survey 2005-2008. Ecosystem Development 2
677 (edited by Hüttl, R.F., Schaaf, W., Biemelt, D., Gerwin, W.), 194 pp.

678 Schachtschabel, P., Heinemann, C.G., 1967. Wasserlösliche Kieselsäure in Lößböden. *Z.*
679 *Pflanzenern. Bodenk.* 118, 22-35.

680 Schlichting, E., Blume, H.P., Stahr, K., 1995. Soils Practical (in German), Blackwell, Berlin,
681 Wien, Germany, Austria.

682 Sommer, M., Kaczorek, D., Kuzyakov, Y., Breuer, J., 2006. Silicon pools and fluxes in soils and
683 landscapes—a review. *J. Plant Nutr. Soil Sci.* 169, 310-329.

684 Sommer, M., Jochheim, H., Höhn, A., Breuer, J., Zagorski, Z., Busse, J., Barkusky, D., Meier, K.,
685 Puppe, D., Wanner, M., Kaczorek, D., 2013. Si cycling in a forest biogeosystem - the
686 importance of transient state biogenic Si pools. *Biogeosciences* 10, 4991-5007.

687 Song, Z., Wang, H., Strong, P. J., Li, Z., Jiang, P., 2012. Plant impact on the coupled terrestrial
688 biogeochemical cycles of silicon and carbon: implications for biogeochemical carbon
689 sequestration. *Earth-Science Reviews* 115, 319-331.

690 Street-Perrott, F. A., Barker, P. A., 2008. Biogenic silica: a neglected component of the
691 coupled global continental biogeochemical cycles of carbon and silicon. *Earth Surface*
692 *Processes and Landforms* 33, 1436-1457.

693 Struyf, E., Conley, D.J., 2012. Emerging understanding of the ecosystem silica filter.
694 *Biogeochemistry* 107, 9-18.

695 Struyf, E., Smis, A., Van Damme, S., Garnier, J., Govers, G., Van Wesemael, B., Conley, D.J,
696 Batelaan, O., Frot, E., Clymans, W., Vandevenne, F., Lancelot, C., Goos, P., Meire, P., 2010.
697 Historical land use change has lowered terrestrial silica mobilization. *Nature*
698 *Communications* 1, 129.

699 Tréguer, P.J., De La Rocha, C.L., 2013. The world ocean silica cycle. *Ann. Rev. Mar. Sci.* 5, 477-
700 501.

701 Tréguer, P., Pondaven, P., 2000. Global change: silica control of carbon dioxide. *Nature* 406,
702 358-359.

703 Vandevenne, F. I., Barão, L., Ronchi, B., Govers, G., Meire, P., Kelly, E. F., Struyf, E., 2015.
704 Silicon pools in human impacted soils of temperate zones. *Global Biogeochemical Cycles* 29,
705 1439-1450.

706 Wanner, M., Elmer, M., 2009. "Hot spots" on a new soil surface – how do testate amoebae
707 settle down? *Acta Protozoologica* 48, 281-289.

708 Wanner, M., Seidl-Lampa, B., Höhn, A., Puppe, D., Meisterfeld, R., Sommer, M., 2016.
709 Culture growth of testate amoebae under different silicon concentrations. *European Journal*
710 *of Protistology* 56, 171-179.

711 Watteau, F., Villemin, G., 2001. Ultrastructural study of the biogeochemical cycle of silicon in
712 the soil and litter of a temperate forest. *European Journal of Soil Science* 52, 385-396.

713 Wilding, L. P., Drees, L. R., 1971. Biogenic opal in Ohio soils. *Soil Science Society of America*
714 *Journal* 35, 1004-1010.

715 Zaplata, M.K., A. Fischer & S. Winter, 2010. Vegetation dynamics, in: Ecosystem
716 development 2 (edited by Schaaf, W., Biemelt, D., Hüttl, R.F.), Brandenburg University of
717 Technology Cottbus-Senftenberg, Germany.

718

719

720

721

722

723

724

Biogeosciences Discuss., https://doi.org/10.5194/bg-2017-177
Manuscript under review for journal Biogeosciences
Discussion started: 20 June 2017

725 **Figures and Figure captions**

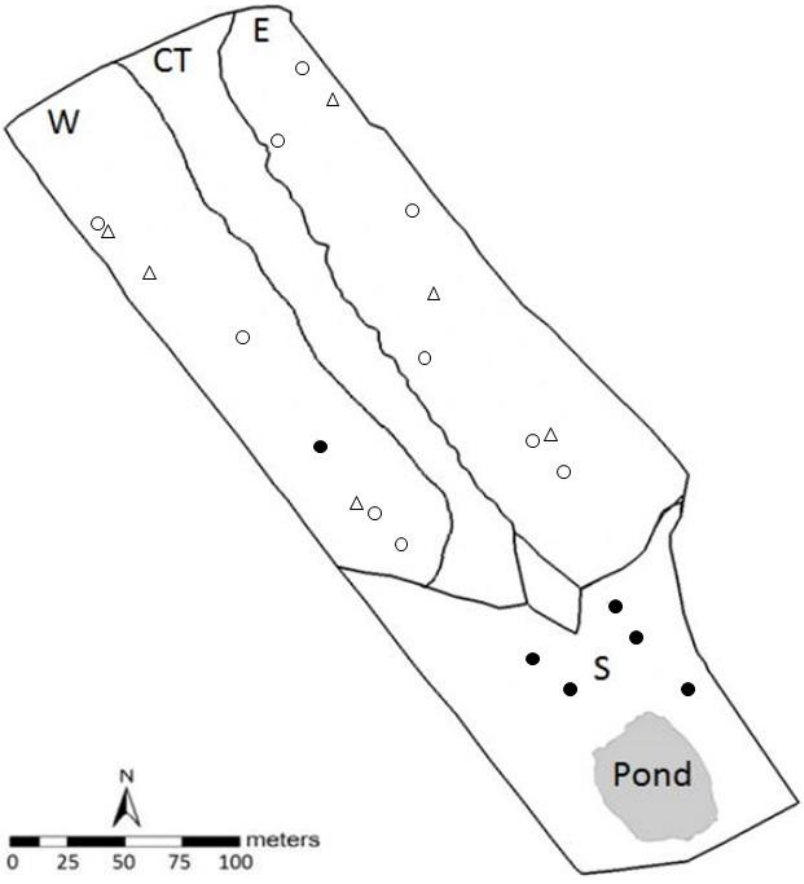

726

727 **Fig. 1.** Map of Chicken Creek (W = western section, CT = central trench, E = eastern section, S
728 = southern section with pond). Triangles indicate the sampling points used for BSi analyses at
729 t_0 (n = 6). Circles indicate the sampling points used for measurements of soil parameters (at
730 t_0 and t_{10}) and plant analyses (only at t_{10}) (W, n = 5; E, n = 6; S, n = 5). Empty and filled circles
731 represent sampling points where *Calamagrostis epigejos* and *Phragmites australis* became
732 dominant. Note that the size of sampling points is not to scale.

Biogeosciences Discuss., https://doi.org/10.5194/bg-2017-177
Manuscript under review for journal Biogeosciences
Discussion started: 20 June 2017

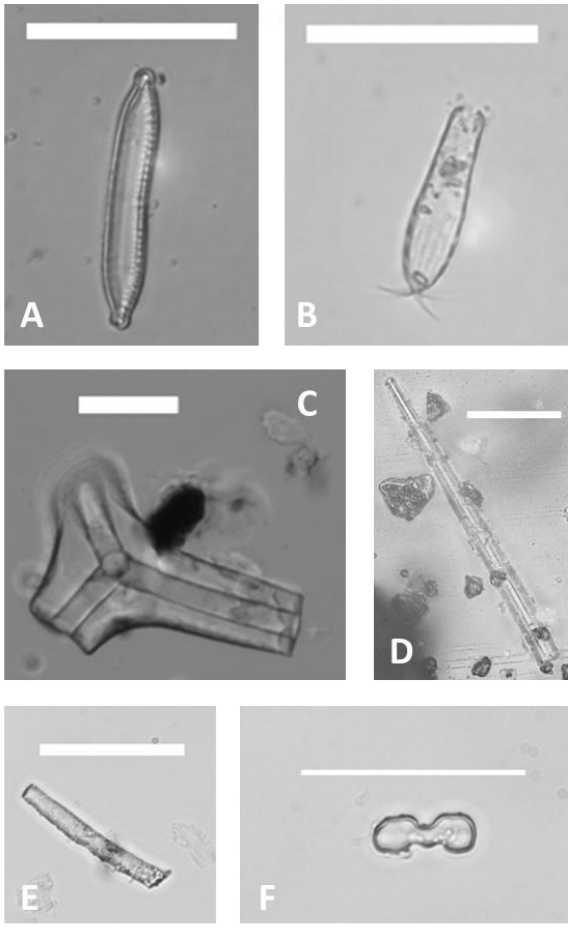

Fig. 2. Micrographs (light microscope) of biogenic silica structures found at Chicken Creek. A) pennate diatom (valve view), B) testate amoeba shell (*Euglypha cristata*), C) and D) sponge spicules (fragments), E) elongate phytolith and F) bilobate phytolith. All scale bars: 50 µm.

Biogeosciences Discuss., https://doi.org/10.5194/bg-2017-177
Manuscript under review for journal Biogeosciences
Discussion started: 20 June 2017

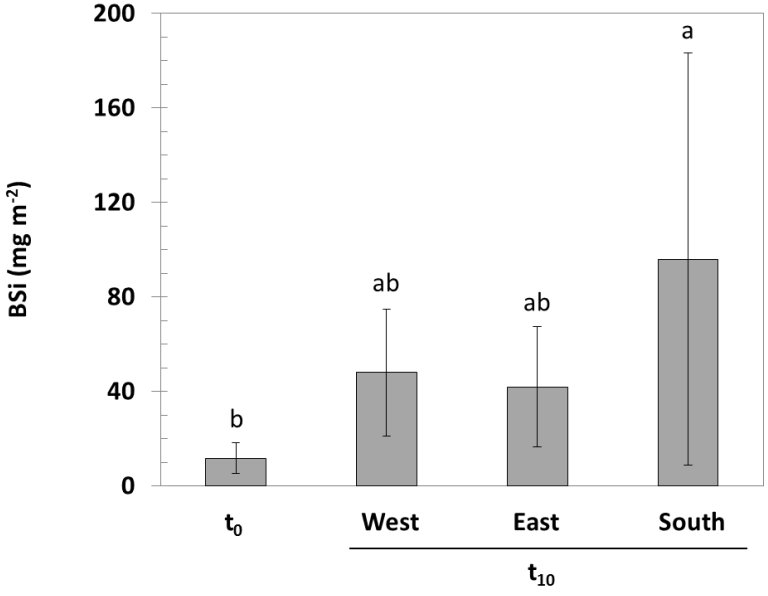

741

742 **Fig. 3.** Total biogenic Si pools in soils (means ± standard deviation, upper 5 cm) at Chicken
743 Creek at the end of construction work (t_0) and after ten years of ecosystem development
744 (western, eastern and southern sections, t_{10}). Significant differences are indicated by
745 different letters ($p < 0.05$, Kruskal-Wallis ANOVA with Dunn's post hoc test).

Biogeosciences Discuss., https://doi.org/10.5194/bg-2017-177
Manuscript under review for journal Biogeosciences
Discussion started: 20 June 2017

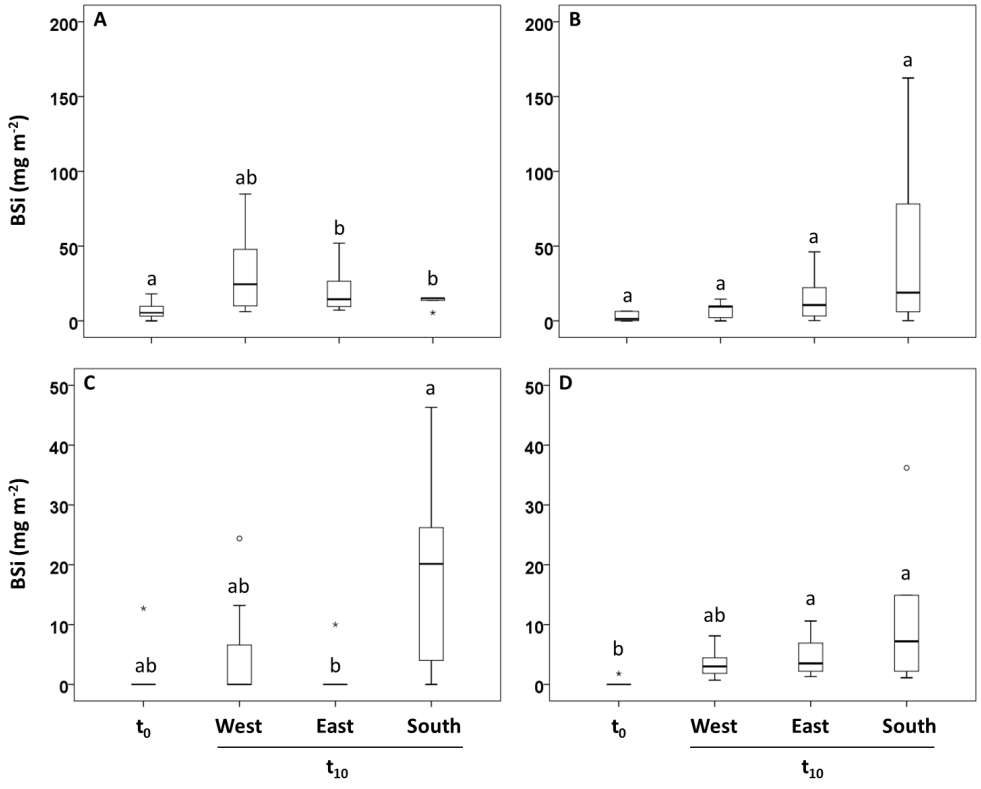

Fig. 4. Boxplots (top, middle and bottom lines of the boxes show the 25th, 50th and 75th percentiles, respectively, and whiskers represent 1.5× the inter-quartile ranges) of biogenic Si pools in soils (upper 5 cm) at Chicken Creek at the end of construction work (t_0) and after ten years of ecosystem development (western, eastern and southern sections, t_{10}). A) Phytogenic Si pools (phytoliths), B) protophytic Si pools (diatom frustules), C) zoogenic Si pools (sponge spicules) and D) protozoic Si pools (testate amoeba shells). Significant differences are indicated by different letters ($p < 0.05$, Kruskal-Wallis ANOVA with Dunn's post hoc test). Circles and asterisks indicate outliers and extreme values, respectively. Note different scales for diagrams A+B and C+D.

Biogeosciences Discuss., https://doi.org/10.5194/bg-2017-177
Manuscript under review for journal Biogeosciences
Discussion started: 20 June 2017

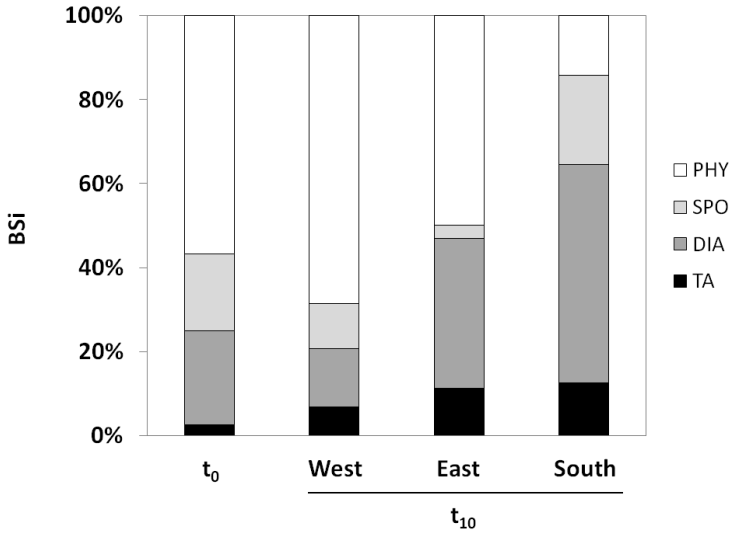

Fig. 5. Proportion of phytoliths (PHY), sponge spicules (SPO), diatom frustules (DIA) and testate amoeba shells (TA) to total BSi in soils (upper 5 cm) at Chicken Creek at t_0 and t_{10}. Note that total BSi pools differ in size (see Fig. 3).

Biogeosciences Discuss., https://doi.org/10.5194/bg-2017-177
Manuscript under review for journal Biogeosciences
Discussion started: 20 June 2017

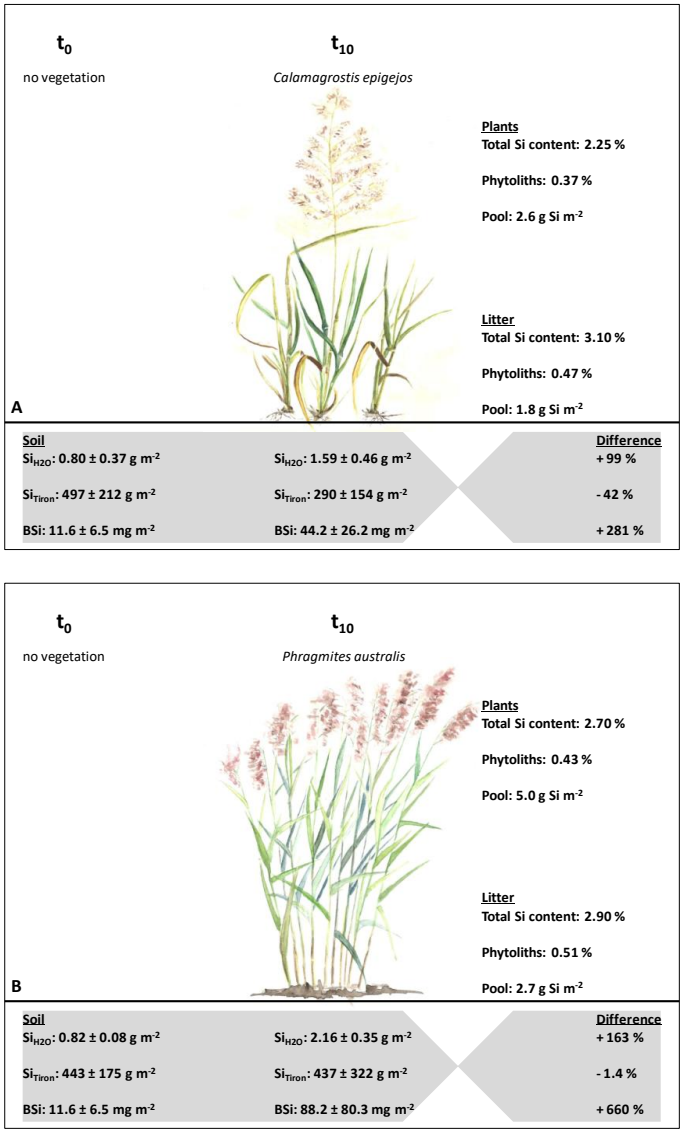

Fig. 6. Comparison of water soluble Si (Si_{H2O}) as well as amorphous Si (Si_{Tiron}) fractions and total BSi in soils (means ± standard deviation, upper 5 cm), where *Calamagrostis epigejos* (A) and *Phragmites australis* (B) became dominant. Data are given for t_0 (no vegetation) and t_{10} (*C. epigejos*, *P. australis*). For t_{10} total Si, phytolith contents and Si pools for *C. epigejos* and *P. australis* (plants and litter) are stated in addition. Paintings from Cornelia Höhn, Müncheberg.

Biogeosciences Discuss., https://doi.org/10.5194/bg-2017-177
Manuscript under review for journal Biogeosciences
Discussion started: 20 June 2017

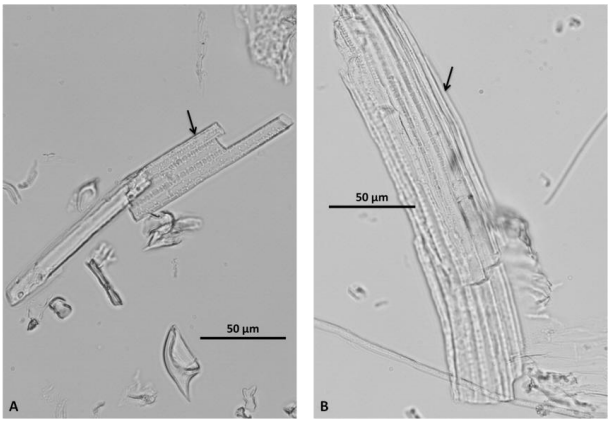

Fig. 7. Micrographs of fragile phytogenic Si structures (arrows) of *C. epigejos* (A) and *P. australis* (B).

Biogeosciences Discuss., https://doi.org/10.5194/bg-2017-177
Manuscript under review for journal Biogeosciences
Discussion started: 20 June 2017

800 **Tables and Table headings**

801

802 **Table 1.** Measured soil parameters (upper 5 cm, means ($\bar{x}$) with standard deviation (SD)) at
803 the different sections of Chicken Creek. Significant differences between t_0 and t_{10} are each
804 stated in bold for the western, eastern and southern section (Mann-Whitney U-test, p
805 <0.05).

Age	Section		Si_{H2O}	Si_{Tiron}	Al_{Tiron}	Fe_{Tiron}	C_{org}	$CaCO_3$	pH
			g m^{-2}						
t_0	West	$\bar{x}$	**0.70**	524	312	249	237	88	**7.9**
		SD	0.10	95	24	33	156	72	0.1
t_{10}	West	$\bar{x}$	**1.73**	552	254	239	556	101	**7.4**
		SD	0.22	300	154	104	167	93	0.1
t_0	East	$\bar{x}$	0.87	**503**	**268**	**261**	**123**	91	**8.1**
		SD	0.48	281	151	130	38	79	0.2
t_{10}	East	$\bar{x}$	1.50	**196**	**122**	**151**	**396**	30	**7.1**
		SD	0.57	49	27	29	54	18	0.2
t_0	South	$\bar{x}$	**0.84**	399	232	238	**160**	174	**8.3**
		SD	0.06	154	112	65	131	109	0.1
t_{10}	South	$\bar{x}$	**2.24**	317	147	157	**474**	126	**7.4**
		SD	0.33	149	62	57	258	40	0.1

806

807

808 **Table 2.** Spearman's rank correlations between measured soil parameters and total BSi
809 (upper 5 cm, n = 6) at Chicken Creek. Significant correlation coefficients are given in bold (p
810 <0.05).

	Si_{H2O}	Si_{Tiron}	Al_{Tiron}	Fe_{Tiron}	C_{org}	$CaCO_3$	pH	BSi
Si_{H2O}	1.000							
Si_{Tiron}	-0.257	1.000						
Al_{Tiron}	-0.600	**0.829**	1.000					
Fe_{Tiron}	-0.486	0.771	**0.943**	1.000				
C_{org}	0.714	0.086	-0.371	-0.486	1.000			
$CaCO_3$	0.200	0.086	-0.086	-0.029	0.029	1.000		
pH	-0.600	0.200	0.486	0.543	-0.771	0.543	1.000	
BSi	**0.941**	-0.213	-0.577	-0.577	**0.880**	0.152	-0.698	1.000

811

Biogeosciences Discuss., https://doi.org/10.5194/bg-2017-177
Manuscript under review for journal Biogeosciences
Discussion started: 20 June 2017

812 **Table 3.** Surface-areas, volumes and surface-to-volume ratios (A/V) of different biogenic
813 siliceous structures found at Chicken Creek.

	Surface-area (µm²)		Volume (µm³)		A/V ratio	
	Min.	Max.	Min.	Max.	Range	Mean (SD)
Bilobate phytoliths	216	3,730	36	2,046	0.7-9.8	2.8 (1.8)
Elongate phytoliths	2,302	22,203	390	14,649	0.6-5.9	2.6 (1.1)
Diatom frustules*	351	9,901	347	28,024	0.3-3.3	0.9 (0.5)
TA shells*	1,229	5,085	900	15,812	0.2-2.7	0.8 (0.7)
Sponge spicules*	305	16,963	291	59,744	0.3-1.6	0.8 (0.4)
Spicule fragments*	2,828	17,268	5,255	34,812	0.5-0.6	0.5 (0.03)

814

815 * Data taken from Puppe et al. (2016).